VERSITA

Central European Journal of **Engineering**

A novel active contour model for unsupervised low-key image segmentation

Jiangyuan Mei[1], Yulin Si[12], Hamid Reza Karimi[2*], Huijun Gao[1]

1   Research Institute of Intelligent Control and Systems,
    Harbin Institute of Technology,
    150080 Harbin, P.R. China

2   Department of Engineering, University of Agder,
    N-4898 Grimstad, Norway

Abstract: Unsupervised image segmentation is greatly useful in many vision-based applications. In this paper, we aim at the unsupervised low-key image segmentation. In low-key images, dark tone dominates the background, and gray level distribution of the foreground is heterogeneous. They widely exist in the areas of space exploration, machine vision, medical imaging, *etc*. In our algorithm, a novel active contour model with the probability density function of gamma distribution is proposed. The flexible gamma distribution gives a better description for both of the foreground and background in low-key images. Besides, an unsupervised curve initialization method is designed, which helps to accelerate the convergence speed of curve evolution. The experimental results demonstrate the effectiveness of the proposed algorithm through comparison with the CV model. Also, one real-world application based on our approach is described in this paper.

Keywords: Image segmentation • Low-key image • Active contour model
             © Versita sp. z o.o.

1.   Introduction

Image segmentation is a fundamental processing step in many image, video and computer vision applications [1]. The objective of image segmentation is to partition an image into a finite number of semantically important regions [2]. In other words, it is the process of assigning pixels into classes such that pixels in the same region share certain visual characteristics [3]. In real-world applications, especially in those control systems based on machine vision, image segmentation is often used to determine or emphasize a certain region of interest in an image, which is a crucial step towards image analysis and digital measurement.

This paper focuses on the segmentation of low-key images, which universally exist in many imaging-based applications such as space telescopes, medical imaging equipment, machine vision systems for process control. Actually, low-key [4] is originally a photography lighting technique, which often accentuates the object only by using only one key light. Therefore, black is the dominant color in a low-key image, and histogram of it has the peaks concentrated along the left side of the graph. A typical low-key image and its histogram are shown in Figure 1.
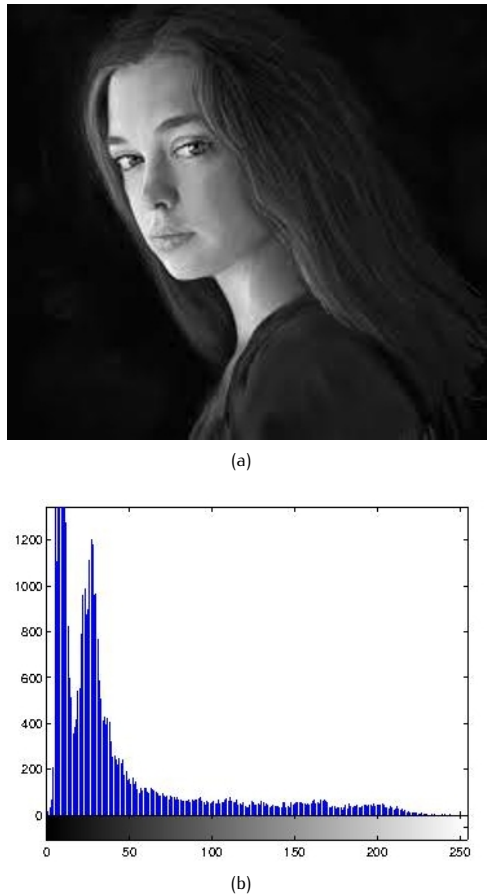
*E-mail: hamid.r.karimi@uia.no

Springer

(a)

(b)

Figure 1. A sample low-key image and its histogram. (a) A typical low-key image. (b) The histogram of (a).

Different from the monotone dark background, the foreground in a low-key image usually has high contrast. This feature brings great difficulty and challenge foreground determination of low-key images. For example, in Figure 1(a), gray level of the main subject varies from hair and clothes to face and neck, resulting in the difficulty of the head portrait segmentation. In other words, the bright skin areas are easy to pick out, but the dark hair and clothes regions are hard to tell from the background.

Although low-key images are mostly produced by professional photographers, they still widely exist in various other applications such like industrial or medical systems. Therefore, an effective low-key image segmentation method is in strong demand. In fact, image segmentation have been extensively studied by researchers. There have been several general-purpose image segmentation algorithms and techniques, such as clustering [5], histogram-based [6], edge detection [7], region-growing [8]. However, they do not perform well on the low-key images, since the gray-level distribution in the foreground is heteroge-

neous. Another effective image segmentation approach is the active contour method, which has been widely studied in recent years. The basic idea of this method is curve evolution, *i.e.* driving the curve towards its interior normal until to the boundary of the object. This process is implemented by energy minimizing with the use of energy functional. According to the type of energy index, existing active contour models can be mainly divided into two categories: edge-based and region-based. Energy functional for edge-based active contour models [9–11] usually contains edge detectors, so it is often used to detect the foreground with the edge defined by strong gradient. Obviously, it not suitable for low-key images. Since the edge-based methods have been found too sensitive to noises and initial curve placement, the region-based active contour models [12–14] become popular. The most famous one is the Chan-Vese (CV) model [12, 13]. However, it is based on the assumption that image intensity values are statistically close to a constant in each separate region, so it is also not much effective for the low-key image segmentation due to the changing gray levels in the foreground area. In order to solve this problem, Shawn Lankton [14] proposed a new active contour framework which utilizes the localizing region-based (LBR) energy. The heterogeneous foreground can be successfully segmented based on the local information with this approach. However, the limitation of the LRB model is that the global minimum result can not be guaranteed by the local energy. Also, it relies on appropriate curve initialization, which is not fit for unsupervised image segmentation. Therefore, the energy index design is of great importance in the active contour method. Still, it has good potential for the unsupervised low-key image segmentation.

In this paper, we propose an unsupervised segmentation algorithm for low-key images based on active contour model, where the energy functional is determined using probability density function (PDF) of the gamma distribution. Meanwhile, an unsupervised curve initialization method is also proposed to shorten the curve evolution process.

The remainder of this paper is organized as follows: In Section 2, steps of the proposed unsupervised low-key image segmentation method are described. In Section 3, experimental results on real-world low-key images are presented. Finally, we draw conclusions and point out future directions in Section 4.

2. Description of the method

In this section, we give a detailed description of the proposed region-based active contour method for low-key im-

age segmentation. Specifically, PDF of the gamma distribution is used in the energy functional. Besides, an unsupervised curve initialization method is presented in this section, aiming to guarantee the converge speed of curve evolution.

2.1. Active contour model with gamma PDF

Given a low-key image $I(x,y)$, the goal of the unsupervised image segmentation is to separate the foreground $f(x,y)$ from the background $b(x,y)$ without human help. Thus the model of a low-key image is described as

$$I(x,y) = l(x,y)f(x,y) + (1-l(x,y))b(x,y), \qquad (1)$$

where $l(x,y)$ is a binary mask to distinguish foreground Ω_f from background Ω_b. The mask is defined as

$$l(x,y) = \begin{cases} 1, & (x,y) \in \Omega_f \\ 0, & (x,y) \in \Omega_b \end{cases}. \qquad (2)$$

As is said above, gray level distribution of Ω_f in a low-key image often centers on a small value, while histogram of Ω_b is much more complex, where some areas in the object are highlighted and some others are in a close tone with the background.

In 1996, Zhu and Yuille [15] proposed a Minimum Description Length (MDL) criterion, which is described as a global energy functional in active contour models. In this criterion, gray level in different regions is consistent with a certain probability distribution $P(I(x,y)|\alpha)$, where α is the parameter. In low-key image segmentation, the foreground Ω_f and background Ω_b are finally separated by an edge curve C. Therefore, the MDL criterion can be expressed as

$$E(C,\{\alpha_i\}) = \mu \int_C ds - \lambda_1 \int_{\Omega_f} \log P(I(x,y)|\alpha_1) dxdy$$
$$- \lambda_2 \int_{\Omega_b} \log P(I(x,y)|\alpha_2) dxdy, \qquad (3)$$

where the positive constants μ, λ_1, λ_2 are weights of these three terms. Minimizing the energy functional by tuning the parameters will finally lead to a meaningful segmentation result.

Many active contour models are based on the MDL criterion, and the most famous one is the CV model. When the Gaussian distribution with a fixed variance, expressed as

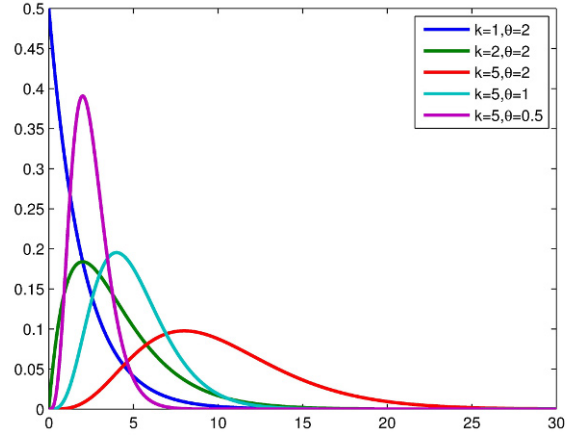$$P(I(x,y)|\alpha_i) = \exp\left(-(I(x,y)-\alpha_i)^2\right), \qquad (4)$$

Figure 2. Gamma PDF with different parameters.

is applied, the MDL criterion will be transformed into the energy functional of the CV model

$$E^{CV}(C,I) = \mu \cdot Length(C)$$
$$- \lambda_1 \int_{inside(C)} |I(x,y)-\alpha_1|^2 dxdy \qquad (5)$$
$$- \lambda_2 \int_{outside(C)} |I(x,y)-\alpha_2|^2 dxdy,$$

where α_1 and α_2 denote the mean intensity values of the foreground and background. The CV model is regarded as one of the most effective active contour models, since the desired global minimum values are obtained with the use of global statistics, and it is not much sensitive to initialization. However, the CV model does not perform well when it deals with the foreground with heterogeneous gray level distribution. This is because the Gaussian PDF is not appropriate to represent the intensity value distribution of low-key images. For instance, as illustrated in Figure 1(b), the histogram is asymmetric and complex with not only one peak in it. Therefore, we choose the flexible gamma PDF to represent the irregular gray-scale distribution of low-key images. It can be expressed in terms of the gamma function parameterized with a shape parameter k and a scale parameter θ, where k and θ are positive values. Gamma PDF with a random variable x is described as

$$P(x|\alpha) = g(x|k,\theta) = \frac{1}{\Gamma(k)} x^{k-1} e^{-x/\theta} \theta^{-k},$$
$$x \geq 0; k, \theta > 0 \qquad (6)$$

where $\Gamma(k) = (k-1)!$. Figure 2 shows some typical shapes of the gamma PDF. Specifically, the shape parameter k controls the distribution shape, while the scale

parameter θ is used to adjust the concentration ratio of the gamma distribution. Since the two-parameter continuous probability distribution is more flexible than Gaussian distribution, it is more suitable to describe the uneven intensity value distribution for low-key images. Choose $\lambda_1 = \lambda_2 = 1$, and the energy functional can be rewritten as follows,

$$
\begin{aligned}
E\left(C,\left\{k_{1,2},\theta_{1,2}\right\}\right) = \mu \int_C ds \\
- \int_{inside(C)} \log\left(g\left(I\left(x,y\right)|k_1,\theta_1\right)\right) dxdy \\
- \int_{outside(C)} \log\left(g\left(I\left(x,y\right)|k_2,\theta_2\right)\right) dxdy.
\end{aligned}
\tag{7}
$$

In other words, two groups of variables should be considered in energy minimizing. One is the parameter set of edge curve C, and the other one, consisting of k and θ, is in the gamma PDF. In [15], Zhu proposed a greedy iterative algorithm to solve the energy minimizing problem. Firstly, keep curve C fixed, then optimize $k_{1,2}$, $\theta_{1,2}$ are to minimize the description cost for both the foreground and background. In the other words, the two parameters in gamma PDF are determined by maximizing the conditional probabilities. Secondly, fix $k_{1,2}$, $\theta_{1,2}$, and minimize the energy index E by evolving the curve C in the steepest direction. Confronting the complexity of the curve evolution description in two-dimensional space, Osher and Sethian [16] introduced the level set method, where the curve C is represented implicitly by a Lipschitz function ϕ. When $C = \{(x,y)|\phi(x,y) = 0\}$, the curve evolution is given by the zero-level curve at time t of the function $\phi(t,x,y)$. Thus the curve evolution has been converted into the three-dimensional space. Using the level set formulation, we describe the energy functional as

$$
\begin{aligned}
E\left(\phi,\left\{k_{1,2},\theta_{1,2}\right\}\right) = \mu \int_\Omega |\nabla H\left(\phi\left(x,y\right)\right)| dxdy \\
- \int_\Omega H\left(\phi\left(x,y\right)\right) \log\left(g\left(I\left(x,y\right)|k_1,\theta_1\right)\right) dxdy \\
- \int_\Omega \left(1 - H\left(\phi\left(x,y\right)\right)\right) \log\left(g\left(I\left(x,y\right)|k_2,\theta_2\right)\right) dxdy,
\end{aligned}
\tag{8}
$$

where $H\left(\phi\left(x,y\right)\right)$ is the Heaviside function, given as

$$
H\left(\phi\left(x,y\right)\right) = \begin{cases} 0 & if \quad \phi\left(x,y\right) \le 0 \\ 1 & if \quad \phi\left(x,y\right) > 0 \end{cases}.
\tag{9}
$$

Therefore, when $k_{1,2}$, $\theta_{1,2}$ are fixed, the evolution of curve C equals to

$$
\frac{\partial \phi}{\partial t} = \delta\phi\left(\log\left(\frac{g\left(I|k_2,\theta_2\right)}{g\left(I|k_1,\theta_1\right)}\right) + div\left(\frac{\nabla\phi}{|\nabla\phi|}\right)\right),
\tag{10}
$$

where $\delta\phi$ is Dirac delta function. Partial differential equation of the Heaviside function is expressed as $\delta\phi = \frac{d}{d\phi}H\left(\phi\right)$.

It should be noted that the curve evolution process may be very slow if the initial curve is placed at a non-ideal place. In the next sub-section, an unsupervised curve initialization method is proposed to deal with this problem.

2.2. Initialization method

An ideal initial curve often evolves quickly to the boundary of the foreground, but a bad one may result in a slow evolution or even failure. Figure 3 illustrates one typical example. A certain initial curve is selected in Figure 3(a), and two gamma distributions are determined with curve fitting in Figure 3(b), red one for foreground and black one for background. The parameters of gamma PDF are calculated as $k_1 = 1.0738$ and $\theta_1 = 36.0705$ for the portrait area, $k_2 = 1.1012$ and $\theta_2 = 33.9568$ for the outside. Eq. (10) suggests that the difference between the two distributions will accelerate the curve evolution speed. In this case, these two distributions almost coincide together, which may lead a slow evolution process.

Here we propose a method to unsupervisedly create the appropriate initial curve. At first, equally divide the low-key image into several regions, and evaluate the mean gray level and variance for each region. Next, due to the low gray-scale value of the background, the regions with the smallest variance and mean value of gray level are chosen as the background. Thus the boundary of these regions is considered as initial curve. Thirdly, in order to further accelerate the curve evolution speed, border of the image is treated as another initial curve. Figure 3(c) shows the initialization result under the proposed method, *i.e.* the left bottom corner is initially regarded as the background. At this time, the gamma-distributed red and black curves in Figure 3(d) for the foreground and background are in totally different shapes, which will lead to a fast curve evolution. The parameters are finally determined as $k_1 = 5.2236$, $\theta_1 = 1.9973$, $k_2 = 1.1285$, $\theta_2 = 37.0896$ respectively.

3. Results and discussion

This section presents the evaluation result of the proposed image segmentation method. The low-key images used in the experiment were obtained from the Internet and selected from the Berkeley Segmentation Data Set and Benchmarks 500 (BSDS500) [17]. The proposed algorithm was implemented in MATLAB 2008b on a computer with 2.00 GHZ CPU and 2 GB RAM. The performance index
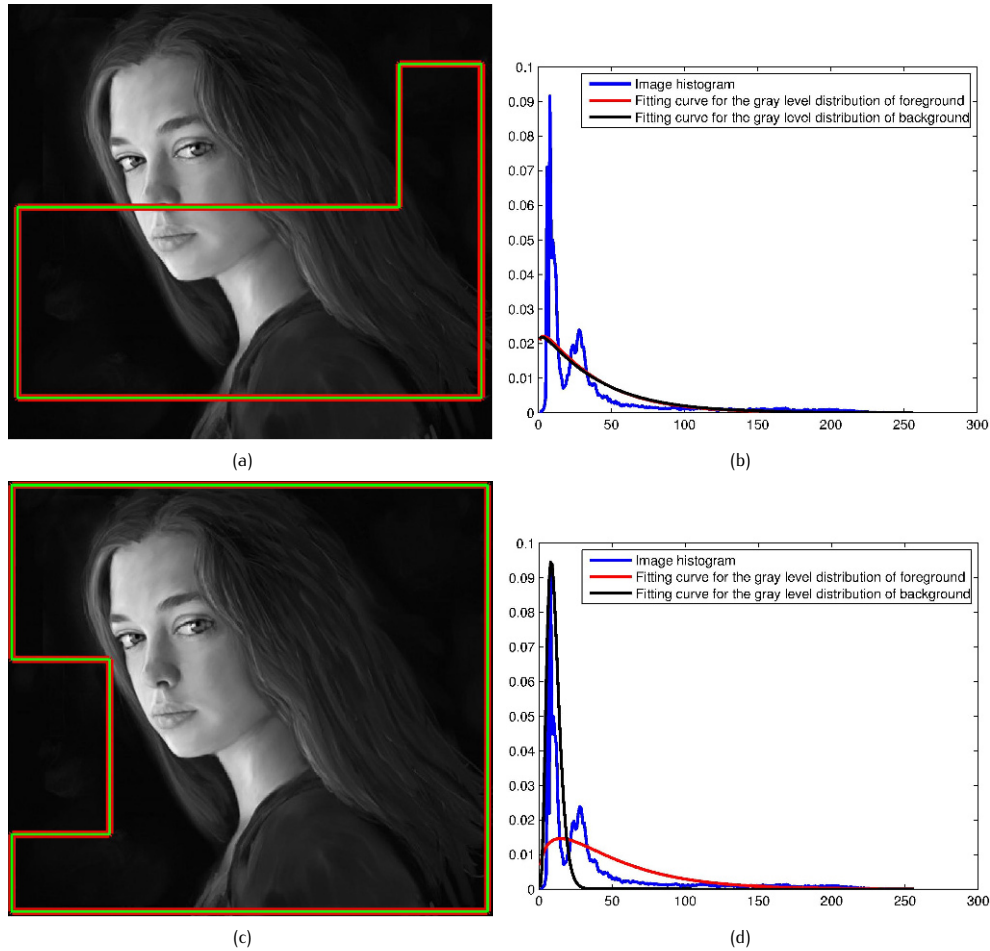
Figure 3. Comparison of different initialization methods. (a) shows a certain initial curve. Under this separation, (b) illustrates the image histogram and the fitting curves for the gray level distribution of foreground and background. The initial curve shown in (c) is obtained by the proposed method, and (d) demonstrates the image histogram, a gentle fitting curve for the intensity value distribution of foreground, and an acuminate one for background.

for evaluation is chosen as the segmentation error rate (SER) [18, 19], defined as

$$e\left(M_{est}, M_{ref}\right) = \frac{\sum_{(x,y)} M_{est}\left(x,y\right) \otimes M_{ref}\left(x,y\right)}{\sum_{(x,y)} M_{ref}\left(x,y\right)}, \qquad (11)$$

where M_{est} is the binary mask for the segmentation result based on the proposed method, and M_{ref} is the manual segmentation result. The symbol of $\otimes$ represents the "XOR" operation.

3.1. Comparison with the CV model

Firstly, comparison is performed between our method and the CV model, and Figure 4 gives the experimental results based on three typical low-key images. The original images, namely Woman, Bird and Flower, Goose are placed in the first column of Figure 4. Images in the second column of Figure 4 are the manual segmentation results. The third column in Fig 4 represents the image segmentation results by using the CV model. Finally, Based on the proposed initialization method and the active contour model with gamma PDF, the segmentation results are obtained, shown in the last column of Fig 4.

It is obvious that the proposed method gives a more accurate and robust segmentation performance for low-key images. It needs to be noted that even the boundaries between background the dark regions in the foreground are detected, which are also difficult in the manual segmentation. However, the CV model is only fit for the boundaries in sharp contrast, such as the contour of the face in Woman. Statistically, data in Table 1 suggest the proposed method has greatly improved the image segmenta-

Figure 4. Demonstration of different unsupervised segmentation approaches on low key images. (a) 4 typical low key images which are chosen from Internet and BSDS500. (b) Manual segmentation results. (c) Segmentation results yielded by CV model [13]. (d) Segmentation results produced by our proposed algorithm.

tion accuracy for low-key images with a relatively lower SER.

Table 1. SER in Performance Comparison

Image	CV model	Proposed method
Woman	0.7120	0.0662
Bird	0.3164	0.0732
Flower	0.6732	0.0951
Goose	0.2632	0.0132

3.2. Application in machine vision

There exist a lot of low-key images in industrial systems based on machine vision. In most cases, in order to guarantee the target detection stability, special light sources need to be introduced into the vision system. This will usually keep the background in a low gray level. At the same time, intensity value distribution of the target is heterogeneous with the existence of shadows and light reflectance. Therefore, these images should be regarded as low-key images. The first column in Figure 5 shows the images of several typical E-shaped magnet in an industrial measurement system. One of the most important processing steps for magnet identification or measurement is the image segmentation process. The second column in Figure 5 illustrates the segmentation result with the use of CV method in this paper. We can see, the rough surface of elements result in the heterogeneous reflection, and CV method is not suitable for dealing with these images. In contrary, our proposed method is good at performing on these industrial images, and the third column in Figure 5 illustrates the segmentation methods by using proposed method. Although noises appear in the background and regions with low gray-scale value exist in the target, the unsupervised low-key image segmentation result is still accurate. Furthermore, we conduct the experiment on an E-shaped magnet image database captured by our devices. The database contains 1026 images, and they are all captured under the industrial circumstance. Table 2 gives the performance comparison of our method with CV
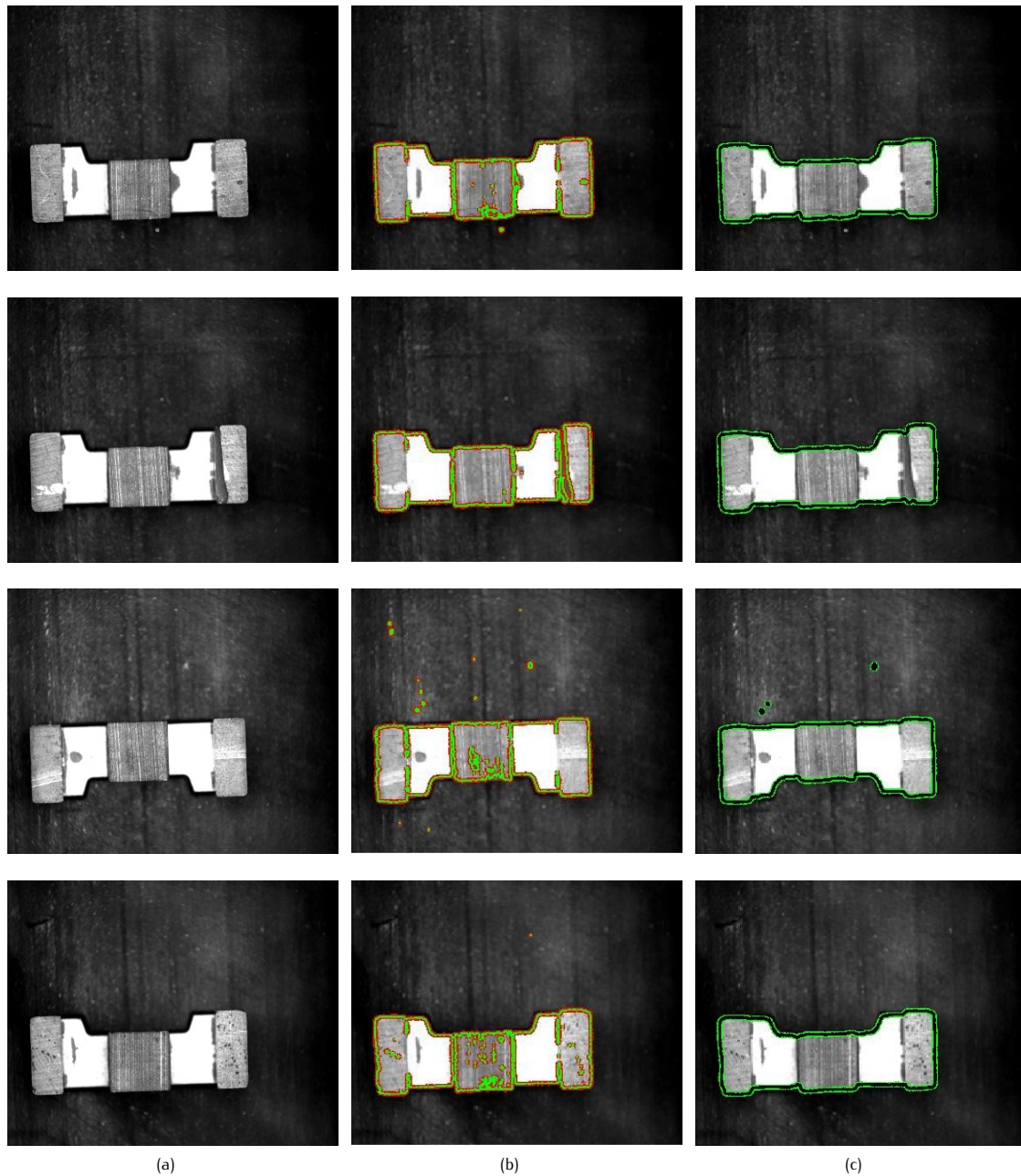
Figure 5. Demonstration of different unsupervised segmentation approaches on E-shaped magnet images. (a) 4 typical E-shaped magnet images. (b) Segmentation results yielded by CV model [13]. (c) Segmentation results produced by our proposed algorithm.

model on the E-shaped magnet images. From the table, we can see our proposed algorithm is more accurate than CV model. It deserves pointing out that the execution efficiency of our framework is the relatively low, as shown in the last column of Table 2. The reason for the low efficiency is that the evaluation of parameters in gamma PDF is more time consuming than Gaussian distribution.

Besides, the programs of our algorithm is coded in Matlab, thus the efficiency of our program would be improved if coded in Java or C++ environment.

Table 2. Performance comparison of different methods on the E-shaped magnet images

Index	CV model	Proposed method
max(SER)	0.4320	**0.2220**
min(SER)	0.0121	**0.0030**
average(SER)	0.0832	**0.0241**
std(SER)	0.1193	**0.0584**
average time	**18s**	23s

4. Conclusions

In this work, we consider the problem of unsupervised segmentation for the low-key images, which exist in various kinds of applications. Low-key images usually contain the foreground with heterogeneous gray-scale distribution and the almost dark background. This feature leads to the problem of image segmentation, where many traditional methods fail.

In this paper, a novel active contour model with the gamma PDF is proposed, and an unsupervised curve initialization method is also presented. The main advantages of our algorithm are as follows. Firstly, this model is established based on the global statistics, so the method seldom plunges into local minimum points. Additionally, due to the asymmetry and flexibility of the gamma PDF, this model is more appropriate for the heterogeneous low-key image segmentation. Finally, the unsupervised initialization method succeeds in accelerating the curve evolution speed.

In the experiment, several illustrative low-key image segmentation examples are given. The classical CV model fails to perform well while the proposed method shows reasonable results. We have also explored the application of the low-key image segmentation in industrial measurement system based on machine vision, and the proposed algorithm arrives at an accurate and robust result.

However, one drawback of this framework is the relatively low execution efficiency, so it is now hard to be fully adopted in the real-world environment without enough optimization. Therefore, further research needs to be carried out on the optimization of the proposed approach.

References

[1] Zhang H., Fritts J., Goldman S., Image segmentation evaluation: A survey of unsupervised methods, Computer Vision and Image Understanding, vol. 110, no. 2, 260–280, 2008

[2] Houhou N., Thiran J., Bresson X., Fast texture segmentation model based on the shape operator and active contour, 2008 IEEE Conf. Computer Vision and Pattern Recognition, 1–8

[3]] Puranik P., Bajaj P., Abraham A., Palsodkar P., et al., Human perception-based color image segmentation using comprehensive learning particle swarm optimization, 2009 2nd Int. Conf. Emerging Trends in Engineering and Technology, 630–635

[4]] Reinhard E., Stark M., Shirley P., Ferwerda J., Photographic tone reproduction for digital images, ACM Transactions on Graphics, vol. 21, no. 3, 267–276, 2002

[5] Lloyd S., Least squares quantization in pcm, IEEE Trans. Information Theory, vol. 28 no. 2, pp. 129–137, 1982

[6] Shapiro L., Stockman G., Computer vision. 2001 (2001)

[7] Lindeberg T., Li M., Segmentation and classification of edges using minimum description length approximation and complementary junction cues, Computer Vision and Image Understanding, vol. 67, no. 1 pp. 88–98, 1997

[8] Adams R., Bischof L., Seeded region growing, IEEE Trans. Pattern Analysis and Machine Intelligence, vol. 16, no. 6, 641–647, 1994

[9] Kass M., Witkin A., Terzopoulos D., Snakes: Active contour models, International Journal of Computer Vision, vol. 1, no. 4, 321–331, 1998

[10] Kichenassamy S., Kumar A., Olver P., Tannenbaum A., et al., Conformal curvature flows: from phase transitions to active vision, Archive for Rational Mechanics and Analysis, vol. 134, no. 3, 275–301, 1996

[11] Caselles V., Kimmel R., Sapiro G., Geodesic active contours, International Journal of Computer Vision, vol. 22, no. 1, 61–79, 1997

[12] Chan T., Sandberg B., Vese L., Active contours without edges for vector-valued images, Journal of Visual Communication and Image Representation, vol. 11, no. 2, 130–141, 2000

[13] Chan T., Vese L., Active contours without edges, IEEE Trans. Image Processing, vol. 10, no. 2, 266–277, 2001

[14] Lankton S., Tannenbaum A., Localizing region-based active contours, IEEE Trans. Image Processing, vol. 17, no. 11 2029–2039, 2008

[15] Zhu S., Yuille A., Region competition: Unifying snakes, region growing, and bayes/mdl for multiband image segmentation, IEEE Trans. Pattern Analysis and Machine Intelligence, vol. 18, no 9, 884–900, 1996

[16] Osher S., Sethian J., Fronts propagating with curvature-dependent speed: algorithms based on

hamilton–jacobi formulations, Journal of Computational Physics, vol. 79, no. 1, 12–49, 1988

[17] Martin D., Fowlkes C., Tal D., Malik J., A database of human segmented natural images and its application to evaluating segmentation algorithms and measuring ecological statistics, in Proc. 8th IEEE Int. Conf. Computer Vision, vol. 2, 416–423, 2001

[18] Kim C., Segmenting a low–depth–of–field image using

morphological filters and region merging, IEEE Trans. Image Processing, vol. 14, no. 10, 1503–1511, 2005

[19] Liu Z., Li W., Shen L., Han Z., et al., Automatic segmentation of focused objects from images with low depth of field, Pattern Recognition Letters, vol. 31, no. 7, 572–581, 2010